PCCP

ROYAL SOCIETY OF CHEMISTRY

PAPER

View Article Online
View Journal | View Issue

Cite this: *Phys. Chem. Chem. Phys.*, 2022, **24**, 13605

A geometric approach to decoding molecular structure and dynamics from photoionization of isotropic samples†

Andres F. Ordonez [ab] and Olga Smirnova [ac]

We propose a geometric approach to the description and analysis of photoelectron angular distributions resulting from isotropic samples in the case of few-photon ionization by electric fields of arbitrary polarization. This approach formulates the standard photoionization observables – the $b_{l,m}$ expansion coefficients of the photoelectron angular distribution, in terms of geometrical properties of the vector field $\vec{D}(\vec{k}) \equiv \langle \vec{k}|\vec{d}|0\rangle$ describing the electronic transition from a bound state $|0\rangle$ into a scattering state $|\vec{k}\rangle$ – the photoionization transition dipole. Besides revealing selection rules for the enantio-sensitivity of $b_{l,m}$ coefficients in multiphoton ionization, our approach yields very compact expressions for both chiral and achiral molecules revealing how the molecular rotational invariants couple to the rotational invariants of the setup defined by the electric field polarization and the arrangement of photoelectron detectors. We apply this approach to one-photon ionization and find that the forward–backward asymmetry parameter $b_{1,0}$, emerging exclusively in chiral molecules and encoded in the field $\vec{B}(\vec{k}) \equiv i\vec{D}^*(\vec{k}) \times \vec{D}(\vec{k})$, is sensitive only to the components of $\vec{D}(\vec{k})$ perpendicular to $\vec{k}$, while the regular asymmetry parameter $b_{2,0}$ emerging in chiral and achiral molecules is sensitive only to the component of $\vec{D}(\vec{k})$ parallel to $\vec{k}$. Next, we analyze resonantly enhanced two-photon ionization and show that $b_{0,0}$ and $b_{1,0}$ can be written in terms of an effectively stretched $\vec{D}(\vec{k})$, and how $b_{1,0}$ and $b_{3,0}$ can be used to probe $\vec{B}(\vec{k})$.

Received 10th December 2021,
Accepted 21st April 2022

DOI: 10.1039/d1cp05645j

rsc.li/pccp

1 Introduction

Photoelectrons provide an important window into the structure of matter and have long been used as a probe of molecular structure in static and time-resolved experiments.[1,2] Photoelectron angular distributions[3] (PADs) encode structural information which goes well beyond the energy spectrum of the molecule, even if the molecule is randomly oriented in space. Chiral molecules present a paramount example of such structural sensitivity: opposite enantiomers of a chiral molecule randomly oriented in space yield markedly different PADs when illuminated with circularly polarized light – a phenomenon known as photoelectron circular dichroism (PECD).[4–8] PECD, with its unusually high enantio-sensitivity, clearly stands out as a tool for exploring structure and dynamics of chiral molecules. It has been studied across a wide range of molecular species[9] and extended to the multi-photon and tunneling ionization regimes.[10–14] Crucially, the extension of PECD into the realm of multiphoton ionization[10,11] provides both access to time-resolved ultrafast enantio-sensitive electronic dynamics[14–17] and the means to control the enantio-sensitive signal observed in the photoelectron angular distributions.[18,19]

The fact that molecular handedness can be inferred from the PAD of a randomly oriented sample raises the following question: *how can we recover the molecular-frame information (not just handedness) encoded in the PAD of randomly oriented molecular samples?* This encoding of molecular-frame information proceeds in several steps: the nuclear configuration is encoded in the electronic wave functions of the ground $|0\rangle$ and scattering states $|\vec{k}\rangle$, these states are subsequently encapsulated into photoionization transition dipoles $\vec{D}(\vec{k}) \equiv \langle \vec{k}|\vec{d}|0\rangle$, and these dipoles are in turn used to calculate the laboratory-frame PAD. The last step requires averaging over molecular orientations and drastically reduces the amount of information contained in the vector field $\vec{D}(\vec{k})$ to a handful of coefficients $b_{l,m}$ describing the laboratory-frame PAD in terms of spherical harmonics $Y_l^m(\hat{k})$ (see *e.g.* ref. 4). So we might as well ask: *what do these few $b_{l,m}$ coefficients tell us about the molecular-frame vector field $\vec{D}(\vec{k})$?* Answering this question is the main objective of this paper.

The standard approach to the computation of molecular $b_{l,m}$ coefficients[4,20–24] provides the connection between molecular

[a] *Max-Born-Institut, 12489 Berlin, Germany. E-mail: olga.smirnova@mbi-berlin.de*
[b] *ICFO-Institut de Ciencies Fotoniques, The Barcelona Institute of Science and Technology, 08860 Castelldefels (Barcelona), Spain. E-mail: andres.ordonez@icfo.eu*
[c] *Technische Universität Berlin, 10623, Berlin, Germany*

† Electronic supplementary information (ESI) available. See DOI: https://doi.org/10.1039/d1cp05645j

and laboratory frame PADs[25–27] and is the basis for the accurate description of PADs in complex polyatomic molecules.[28] However, it does not provide a simple answer to our question. This motivated the development of the alternative approach to the analysis of PADs presented here.

Our approach provides insightful connections between the $b_{l,m}$ coefficients and the photoionization dipole vector field $\vec{D}(\vec{k})$. A previous version of this approach limited to $b_{0,0}$ and $b_{1,0}$ has already proven to be very useful for photoionization of chiral molecules (see ref. 17 and 29). We expect the general version provided here to be useful beyond chiral molecules and throughout the field of molecular photoionization for comparison of different non-linear signals generated due to fields with complex geometries.

In particular, we applied this alternative approach to the cases of one- and two-photon resonantly-enhanced ionization of randomly oriented molecules and found that the $b_{l,m}$ coefficients encode concrete geometrical information about $\vec{D}(\vec{k})$ and about the associated field $\vec{B}(\vec{k}) \equiv i\vec{D}^*(\vec{k}) \times \vec{D}(\vec{k})$, which plays a central role in the photoionization of chiral molecules.[29,30] The geometrical character of our findings suggests potential connections to geometrical and topological properties[31,32] in other research fields such as structured light,[33–36] magnetism,[37] and electron dynamics in crystals.[38]

Another fundamental aspect we address here is that due to the isotropic distribution of molecular orientations, the observables can only depend on rotational invariants (RIs), *i.e.* on quantities independent of the molecular orientation, such as the angle between two transition dipoles, or the angle between the photon spin and the z axis defined by the photoelectron detection setup. This is in fact a common feature enabling meaningful comparisons across different enantio-sensitive methods working in diverse detection regimes with isotropic samples, from microwave excitation to optical wave-mixing to photoionization and standard absorption circular dichroism and optical activity.[17] The RIs are divided into those describing the molecule – molecular RIs, and those describing the light and detection setup – setup RIs. The observables, here the $b_{l,m}$ coefficients, must therefore be functions of those two groups of RIs. Our approach provides these functions, which we show to be linear both in the molecular and in the setup RIs, and thus reveals how the molecular RIs are coupled to the setup RIs. The understanding of this coupling is very relevant for schemes looking for effective ways of maximizing the enantio-sensitive response,[19] a highly non-trivial task for multi-color fields of arbitrary polarization.

The paper is organized as follows. Section 2 describes the idea of our approach in simple terms, summarizing the key technical steps of Section 3. The latter is complemented by further mathematical details in the ESI.† Section 4 contains the analysis of local properties of $b_{l,m}$ coefficients and the underlying vector fields relevant to one-photon ionization. Sections 2–4 are relevant for both chiral and achiral molecules subject to electric fields of arbitrary polarization. Section 5 explores PECD in two-photon resonantly-enhanced ionization of chiral molecules and provides the first steps towards the ambitious goal of reconstructing $\vec{B}(\vec{k}) \equiv i\vec{D}^*(\vec{k}) \times \vec{D}(\vec{k})$[29,30] from the $b_{l,m}$ coefficients. Section 6 concludes the work. Further applications of the approach presented here can be found in ref. 29 and 39.

2 Idea of the method

The interpretation of molecular structure and dynamics probed *via* photoionization of randomly oriented samples usually relies on a mathematical formulation employing a partial wave expansion of the scattering wave function, which is normally performed at the outset of any PAD derivation[4,20,24,40,41] before the orientation averaging step. This traditional approach yields $b_{l,m}$ coefficients in a form in which it is not clear how the geometric properties of $\vec{D}(\vec{k})$ are encoded in $b_{l,m}$. For example, in chiral molecules, this approach obscures the connection between $b_{1,0}$ (describing PECD) and the geometry of $\vec{D}(\vec{k})$ beyond the fact that $b_{1,0}$ results from complex interference of *many* (about 15, see ref. 41–45) partial waves.

The key idea of the approach we present here is that it is possible to obtain analytical expressions for the $b_{l,m}$ coefficients without invoking any type of expansion for the scattering wave function. These expressions reveal the link between $b_{l,m}$ and $\vec{D}(\vec{k})$ and show how the geometry of the vector field $\vec{D}(\vec{k})$ maps into the $b_{l,m}$ coefficients.

In particular, we found a way to perform the orientation averaging step without expanding the scattering wave function. To achieve this it is important to identify the natural frame of reference of each vector involved in the photoionization process. As usual, the natural frame of reference of transition dipoles is the molecular frame, while that of the electric fields and laboratory axes is the laboratory frame. For the photoelectron momentum, identifying the natural reference frame is less straightforward. Indeed, while the photoelectron momentum $\vec{k}$ is detected in the laboratory frame and keeping it in this frame throughout PAD derivations is the usual practice,[4] its natural frame of reference is the molecular frame. This is because $\vec{k}$ labels the electronic scattering wave function, which, like the bound electronic wave functions, is fixed in the molecular frame. Fig. 1 illustrates that scattering states having the same $\vec{k}$ in the *laboratory* frame ($\vec{k}_1$ and $\vec{k}_2'$) but corresponding to

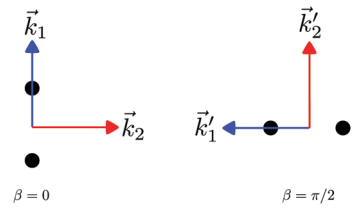

Fig. 1 Two orientations of a diatomic molecule. The black circles indicate the nuclei. The scattering state depends on the relative angle between the molecular axis and the propagation direction $\vec{k}$ of the outgoing (asymptotically plane) wave. Therefore, while the states $|\vec{k}_1\rangle$ and $|\vec{k}_1'\rangle$ satisfying $\vec{k}_1^{\mathrm{M}} = \vec{k}_1'^{\mathrm{M}}$ are related to each other by a simple rotation, the states $|\vec{k}_1\rangle$ and $|\vec{k}_2'\rangle$ satisfying $\vec{k}_1^{\mathrm{L}} = \vec{k}_2'^{\mathrm{L}}$ are not related to each other in any simple way.

different molecular orientations are not related to each other in any simple way, while scattering states having the same $\vec{k}$ in the *molecular* frame ($\vec{k}_1$ and $\vec{k}_1'$) are related to each other *via* a simple rotation of their wave functions.

The desire of keeping each vector in its natural reference frame and of relying on the techniques for orientation averaging of tensors[46] will dictate the sequence of steps described in the next section. This sequence yields expressions for the $b_{l,m}$ coefficients as products of molecular RIs and setup RIs, or in general, as sums of such products.

We shall see that the molecular RIs will be represented in terms of $\vec{k}$-dependent molecular vector fields. Such fields are unique to every molecule and encode its structure. Thus, the key differences of our approach from the standard approach are (i) avoiding partial wave expansion of scattering states, (ii) keeping the photoelectron momentum $\vec{k}$ in the molecular frame, and (iii) exchanging the order of integrals over the molecular orientations and over the orientations of $\vec{k}$. This approach reveals physics that are otherwise obscured by the partial wave expansion. Naturally, the standard expressions can also be recovered from our representation. Note that we are not suggesting that our approach allows the numerical calculation of the $b_{l,m}$ coefficients without doing a partial wave expansion. The partial wave expansion may still be needed for the computation of $\vec{D}(\vec{k})$, but what we are interested in is the connection between $b_{l,m}$ and $\vec{D}(\vec{k})$, not the calculation of $\vec{D}(\vec{k})$ itself.

3 General methodology

The photoionization of an isotropic molecular sample results in a photoelectron spectrum $W^{\mathrm{L}}(\vec{k}^{\mathrm{L}})$ given by

$$W^{\mathrm{L}}(\vec{k}^{\mathrm{L}}) = \int \mathrm{d}\rho\, W^{\mathrm{L}}(\vec{k}^{\mathrm{L}}, \rho), \tag{1}$$

where $W^{\mathrm{L}}(\vec{k}^{\mathrm{L}}, \rho)$ is the photoelectron spectrum for a given molecular orientation $\rho \equiv \alpha\beta\gamma$, $\alpha\beta\gamma$ are the Euler angles, $\int \mathrm{d}\rho \equiv \frac{1}{8\pi^2}\int_0^{2\pi}\mathrm{d}\alpha\int_0^{\pi}\mathrm{d}\beta\int_0^{2\pi}\mathrm{d}\gamma$ is the integral over all molecular orientations, and the superscript L indicates vectors and functions in the laboratory frame. Since we can always expand $W^{\mathrm{L}}(\vec{k}^{\mathrm{L}})$ into real spherical harmonics‡ $\tilde{Y}_l^m(\hat{k}^{\mathrm{L}})$,

$$W^{\mathrm{L}}(\vec{k}^{\mathrm{L}}) = \sum_{l,m} \tilde{b}_{l,m}(k)\, \tilde{Y}_l^m(\hat{k}^{\mathrm{L}}), \tag{2}$$

then any information about the molecule and the ionizing field encoded in the photoelectron spectrum $W^{\mathrm{L}}(\vec{k}^{\mathrm{L}})$ is now neatly summarized in the expansion coefficients $\tilde{b}_{l,m}(k)$,

$$\begin{aligned}\tilde{b}_{l,m}(k) &= \int \mathrm{d}\Omega_k^{\mathrm{L}}\, \tilde{Y}_l^m(\hat{k}^{\mathrm{L}}) W^{\mathrm{L}}(\vec{k}^{\mathrm{L}}),\\ &= \int \mathrm{d}\Omega_k^{\mathrm{L}}\, \tilde{Y}_l^m(\hat{k}^{\mathrm{L}}) \int \mathrm{d}\rho\, W^{\mathrm{L}}(\vec{k}^{\mathrm{L}}, \rho),\end{aligned} \tag{3}$$

where $\int \mathrm{d}\Omega_k^{\mathrm{L}} \equiv \int_0^{\pi}\mathrm{d}\theta_k^{\mathrm{L}}\int_0^{2\pi}\mathrm{d}\phi_k^{\mathrm{L}}\sin\theta_k^{\mathrm{L}}$, $\hat{k}^{\mathrm{L}} = (1, \theta_k^{\mathrm{L}}, \phi_k^{\mathrm{L}})$ in spherical coordinates, and $\vec{k}^{\mathrm{L}} = k\hat{k}^{\mathrm{L}}$. Measured as well as calculated values for these coefficients for particular systems can be found for example in ref. 7, 25, 26 and 47–51.

Following the definition of a rotated function (see *e.g.* ref. 52), the photoelectron spectrum in the molecular frame is given by the relation $W^{\mathrm{M}}(\vec{k}^{\mathrm{M}}, \rho) = W^{\mathrm{L}}(\vec{k}^{\mathrm{L}}, \rho)$, or equivalently $W^{\mathrm{M}}(S^{-1}(\rho)\vec{k}^{\mathrm{L}}, \rho) = W^{\mathrm{L}}(\vec{k}^{\mathrm{L}}, \rho)$, where $\vec{k}^{\mathrm{L}} = S(\rho)\vec{k}^{\mathrm{M}}$ and $S(\rho)$ is the rotation matrix that takes vectors from the molecular to the laboratory frame and the superscript M indicates vectors and functions in the molecular frame. This means that

$$\begin{aligned}\tilde{b}_{l,m}(k) &= \int \mathrm{d}\Omega_k^{\mathrm{L}}\, \tilde{Y}_l^m\left(\hat{k}^{\mathrm{L}}\right) \int \mathrm{d}\rho\, W^{\mathrm{M}}\left(S^{-1}(\rho)\vec{k}^{\mathrm{L}}, \rho\right),\\ &= \int \mathrm{d}\rho \int \mathrm{d}\Omega_k^{\mathrm{L}}\, \tilde{Y}_l^m(\hat{k}^{\mathrm{L}}) W^{\mathrm{M}}\left(S^{-1}(\rho)\vec{k}^{\mathrm{L}}, \rho\right),\end{aligned} \tag{4}$$

where in the second line we exchanged the integration order because we want to make the change of variables $\vec{k}^{\mathrm{M}} = S^{-1}(\rho)\vec{k}^{\mathrm{L}}$, which only exists inside the integral over orientations and yields

$$\begin{aligned}\tilde{b}_{l,m}(k) &= \int \mathrm{d}\rho \int \mathrm{d}\Omega_k^{\mathrm{M}}\, \tilde{Y}_l^m(S(\rho)\hat{k}^{\mathrm{M}}) W^{\mathrm{M}}(\vec{k}^{\mathrm{M}}, \rho),\\ &= \int \mathrm{d}\Omega_k^{\mathrm{M}} \int \mathrm{d}\rho\, \tilde{Y}_l^m(S(\rho)\hat{k}^{\mathrm{M}}) W^{\mathrm{M}}(\vec{k}^{\mathrm{M}}, \rho),\end{aligned} \tag{5}$$

where in the second line we exchanged the integration order again because now $\vec{k}^{\mathrm{M}}$ is an integration variable independent of ρ. At this point two questions arise: Why would we want to have the photoelectron momentum in the molecular frame instead of having it in the laboratory frame, where the photoelectron is actually measured? And why would we prefer to do the integral over orientations in eqn (5) instead of the apparently simpler integral over orientations in eqn (3)? The answer to both questions has to do with the form that the photoelectron spectrum $W^{\mathrm{M}}(\vec{k}^{\mathrm{M}}, \rho)$ takes in the case of ionization in the perturbative regime.

As an example, let's consider the simple scenario depicted in Fig. 2: two-photon absorption with a single color field in a three-level system where the two lower levels are bound and

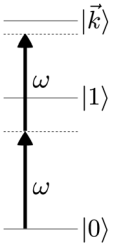

Fig. 2 Excitation scheme for resonantly enhanced photoionization.

‡ We will use tildes to distinguish the real spherical harmonics $\tilde{Y}_{l,m}$ from the usual complex spherical harmonics $Y_{l,m}$ (see ESI†). For $m = 0$ we will omit the tilde.

non-degenerate and the higher level is an infinitely degenerate scattering state. For a Gaussian pulse with central frequency ω_L and spectral width γ the field can be written as

$$\vec{E}(\omega) = \sqrt{2\pi}\left[\frac{\vec{F}_{\omega_L}}{2}\delta_\gamma(\omega-\omega_L) + \frac{\vec{F}^*_{\omega_L}}{2}\delta_\gamma(\omega+\omega_L)\right], \quad (6)$$

where $\delta_\gamma(\omega) \equiv e^{-\omega^2/(2\gamma^2)}\Big/\sqrt{2\pi\gamma^2}$ and the resulting second-order contribution to the probability amplitude of the scattering state $|\vec{k}^M\rangle$ reads as

$$a^{(2)}_{\vec{k}^M}(\rho) = A^{(2)}\left(\vec{d}^L_{\vec{k}^M,1}\cdot\vec{F}^L_{\omega_L}\right)\left(\vec{d}^L_{1,0}\cdot\vec{F}^L_{\omega_L}\right), \quad (7)$$

where $\vec{d}_{i,j} \equiv \langle i|\vec{d}|j\rangle$ is the transition dipole matrix element and $A^{(2)}$ is a function of the difference of the level spacings $\omega_{k1}-\omega_{10}$, the total detuning $2\Delta = \omega_{k0} - 2\omega_L$, and the spectral width γ, $\omega_{ij} \equiv \omega_i - \omega_j$, ω_i is the energy of the state $|i\rangle$, and the superscript (2) indicates the order of the process. The photoelectron spectrum in the molecular frame then reads as

$$W^M(\vec{k}^M,\rho) \equiv \left|a^{(2)}_{\vec{k}^M}\right|^2 = \left|A^{(2)}\right|^2\left(\vec{d}^{L*}_{\vec{k}^M,1}\cdot\vec{F}^{L*}_{\omega_L}\right)\left(\vec{d}^{L*}_{1,0}\cdot\vec{F}^{L*}_{\omega_L}\right) \times\left(\vec{d}^L_{\vec{k}^M,1}\cdot\vec{F}^L_{\omega_L}\right)\left(\vec{d}^L_{1,0}\cdot\vec{F}^L_{\omega_L}\right), \quad (8)$$

where the ρ dependence is implicit in the transition dipoles according to $\vec{d}^L_{i,j} = S(\rho)\vec{d}^M_{i,j}$ [see eqn (7)]. Replacing in eqn (5) we obtain

$$\tilde{b}^{(2)}_{l,m}(k) = \left|A^{(2)}\right|^2\int d\Omega^M_k\int d\rho\,\tilde{Y}^m_l(\hat{k}^L)\left(\vec{d}^{L*}_{\vec{k}^M,1}\cdot\vec{F}^{L*}_{\omega_L}\right)\left(\vec{d}^{L*}_{1,0}\cdot\vec{F}^{L*}_{\omega_L}\right) \times\left(\vec{d}^L_{\vec{k}^M,1}\cdot\vec{F}^L_{\omega_L}\right)\left(\vec{d}^L_{1,0}\cdot\vec{F}^L_{\omega_L}\right). \quad (9)$$

Note that when written in component form, the product of four transition dipole vectors (tensors of rank 1) in this expression forms irreducible spherical tensors of rank μ up to 4 (twice the number of photons N exchanged with the field) which transform according to the Wigner matrix $\mathscr{D}^{(\mu)}(\rho)$. Similarly, the real spherical harmonic $\tilde{Y}^m_l(\hat{k}^L)$ is a superposition of two spherical tensors of rank l that transform according to $\mathscr{D}^{(l)}(\rho)$.[52] Then, from eqn (9) and the orthogonality relation of the Wigner matrices[52] it is evident that the $\tilde{b}^{(2)}_{l,m}$ coefficients with $l > l_{max} = 4$ (in general $l_{max} = 2N$) vanish, as is well known. Expressions analogous to eqn (9) can be obtained for the case of fields with multiple frequencies. In the case of terms $\tilde{b}^{(N_1,N_2)}_{l,m}$ resulting from the interference of pathways involving N_1 and N_2 photons we get $l_{max} = N_1 + N_2$.

If instead of relying on the Wigner matrices to perform the orientation averaging we take into account that the spherical harmonics in eqn (9) are just polynomials of k^L_x/k, k^L_y/k, and k^L_z/k, then $\tilde{b}_{l,m}$ becomes a sum of terms of the form

$$\int d\Omega^M_k\int d\rho\left(\hat{k}^L\cdot\hat{x}^L\right)^p\left(\hat{k}^L\cdot\hat{y}^L\right)^q\left(\hat{k}^L\cdot\hat{z}^L\right)^r \times\left(\vec{d}^{L*}_{\vec{k}^M,1}\cdot\vec{F}^{L*}_{\omega_L}\right)\left(\vec{d}^{L*}_{1,0}\cdot\vec{F}^{L*}_{\omega_L}\right)\left(\vec{d}^L_{\vec{k}^M,1}\cdot\vec{F}^L_{\omega_L}\right)\left(\vec{d}^L_{1,0}\cdot\vec{F}^L_{\omega_L}\right), \quad (10)$$

where $p + q + r \leq l$ and $p + q + r$ has the same parity as l. The vectors in this expression are of two types. The set $\left\{\hat{x}^L,\hat{y}^L,\hat{z}^L,\vec{F}^L_{\omega_L}\right\}$ is fixed in the laboratory frame, while the set $\left\{\hat{k}^M,\vec{d}^M_{\vec{k}^M,1},\vec{d}^M_{1,0}\right\}$ (which appears in the expression above rotated into the laboratory frame $\vec{v}^L = S(\rho)\vec{v}^M$) is fixed in the molecular frame. We take $\hat{k}^M$ fixed in the molecular frame because $\hat{k}^M$ is the quantum label that characterizes the scattering state $|\vec{k}^M\rangle$, which (like the bound states) is fixed in the molecular frame (see *e.g.* Fig. 1). Eqn (10) has the form we wanted to achieve, it is a product of scalar products between vectors fixed in the molecular frame and vectors fixed in the laboratory frame. In this form the integration over orientations can be performed at once applying the technique in ref. 46, which yields a result of the form $\sum_{i,j} g_i M_{ij} f_j$, where the g_i are rotational invariants (RIs) formed with the set of vectors fixed in the molecular frame, the f_j are RIs formed by the set of vectors fixed in the laboratory frame, and the M_{ij} are constants coupling both sets of RIs. Examples of such invariants will be given in the next section.

The structure of the RIs (see ref. 46) and the fact that eqn (10) involves only polar vectors allows us to conclude that if the number of dot products in eqn (10) is odd (even) then the RIs are pseudoscalars (scalars). This means that enantio-sensitivity can only be observed in coefficients $\tilde{b}^{(N)}_{l,m}$ such that l is odd, in agreement with previous works (see *e.g.* ref. 10 and 53). *More interestingly, for coefficients $\tilde{b}^{(N_1,N_2)}_{l,m}$ resulting from interference between pathways with N_1 and N_2 photons, the condition for enantio-sensitivity is that $l + N_1 + N_2$ is odd. That is, if $N_1 + N_2$ is odd, coefficients $\tilde{b}^{(N_1,N_2)}_{l,m}$ with even l can be enantio-sensitive*, in agreement with the recent works in ref. 18 and 54. This is a general condition independent of the polarization of the field and of the photon energies and will be explored in more detail in ref. 39.

Now we will discuss two elementary applications of our methodology. First, we will derive the expression for the $b^{(1)}_{l,m}$ coefficients in one-photon ionization and discuss the molecular information they reveal. Afterwards we will derive and discuss the expressions for the $b^{(2)}_{0,0}$, $b^{(2)}_{1,0}$, and $b^{(2)}_{3,0}$ coefficients relevant for PECD in two-photon ionization. Note that the expressions for $b^{(1)}_{0,0}$ and $b^{(1)}_{1,0}$ coefficients in one-photon ionization and the $b^{(2)}_{1,0}$ coefficient in two-photon ionization have already been derived using a less general procedure in ref. 17.

4 The photoionization dipole field and the $b_{l,m}$ coefficients in one-photon ionization

For the field in eqn (6), the first-order amplitude of the scattering state $|\vec{k}^M\rangle$ reads as

$$a^{(1)}_{\vec{k}^M} = A^{(1)}\left(\vec{D}^L\cdot\vec{F}^L_{\omega_L}\right), \quad A^{(1)} = i\pi\delta_\gamma(\omega-\omega_L), \quad (11)$$

where we use the shorthand notations $\vec{D}^M \equiv \vec{d}^M_{\vec{k}^M,0}$, $\vec{F}^L \equiv \vec{F}^L_{\omega_L}$, and as usual $\vec{D}^L = S(\rho)\vec{D}^M$. From here on, we must keep in mind that $\vec{D}^M = \vec{D}^M(\vec{k}^M)$ is a complex vector field that depends on $\vec{k}^M$.

That is, for a fixed initial state $|0\rangle$, $\vec{D}^{\mathrm{M}}(\vec{k}^{\mathrm{M}})$ is a mapping from the space of real three-dimensional vectors $\vec{k}^{\mathrm{M}} \in \mathbb{R}^3$ to the space of complex three-dimensional vectors $\vec{D}^{\mathrm{M}} \in \mathbb{C}^3$. From eqn (11) it is clear that this complex vector field fully determines the response of the molecule to the ionizing field and therefore the coefficients $\tilde{b}^{(1)}_{l,m}$ must correspond to properties of this vector field. The question is: *which property of the photoionization vector field $\vec{D}^{\mathrm{M}}(\vec{k}^{\mathrm{M}})$ is reflected in a given $\tilde{b}^{(1)}_{l,m}$ coefficient?*

Since for first order amplitudes all frequencies act separately and the most general polarization of a single frequency is elliptical, we will assume an electric field that is elliptically polarized in the xy plane with its major axis along either the $\hat{x}^{\mathrm{L}}$ or the $\hat{y}^{\mathrm{L}}$ axis. From symmetry it follows that the only non-zero $\tilde{b}^{(1)}_{l,m}$ coefficients are $b^{(1)}_{0,0}$, $b^{(1)}_{1,0}$, $b^{(1)}_{2,0}$, $\tilde{b}^{(1)}_{2,2}$, and $\tilde{b}^{(1)}_{2,-2}$ (we omit the tilde for $m = 0$). With the help of eqn (5) and (10), and performing the orientation integrals according to ref. 46 we obtain§ (see ESI†)

$$b^{(1)}_{0,0}(k) = \left|A^{(1)}\right|^2 \left\{\frac{1}{3\sqrt{4\pi}}\int \mathrm{d}\Omega^{\mathrm{M}}_k \left|\vec{D}^{\mathrm{M}}\right|^2\right\}\left\{\left|\vec{F}^{\mathrm{L}}\right|^2\right\}, \tag{12}$$

$$\begin{aligned} b^{(1)}_{1,0}(k) &= \left|A^{(1)}\right|^2 \left\{\frac{1}{6}\sqrt{\frac{3}{4\pi}}\int \mathrm{d}\Omega^{\mathrm{M}}_k \left[\hat{k}^{\mathrm{M}} \cdot \left(\vec{D}^{\mathrm{M}*} \times \vec{D}^{\mathrm{M}}\right)\right]\right\} \\ &\quad \times \left\{\hat{z}^{\mathrm{L}} \cdot \left(\vec{F}^{\mathrm{L}*} \times \vec{F}^{\mathrm{L}}\right)\right\}, \end{aligned} \tag{13}$$

$$\begin{aligned} b^{(1)}_{2,0}(k) &= \left|A^{(1)}\right|^2 \left\{\frac{1}{12\sqrt{5\pi}}\int \mathrm{d}\Omega^{\mathrm{M}}_k \left(3\left|\hat{k}^{\mathrm{M}} \cdot \vec{D}^{\mathrm{M}}\right|^2 - \left|\vec{D}^{\mathrm{M}}\right|^2\right)\right\} \\ &\quad \times \left\{3\left|\hat{z}^{\mathrm{L}} \cdot \vec{F}^{\mathrm{L}}\right|^2 - \left|\vec{F}^{\mathrm{L}}\right|^2\right\}, \end{aligned} \tag{14}$$

$$\begin{aligned} \tilde{b}^{(1)}_{2,2}(k) &= \left|A^{(1)}\right|^2 \left\{\frac{1}{4\sqrt{15\pi}}\int \mathrm{d}\Omega^{\mathrm{M}}_k \left(3\left|\hat{k}^{\mathrm{M}} \cdot \vec{D}^{\mathrm{M}}\right|^2 - \left|\vec{D}^{\mathrm{M}}\right|^2\right)\right\} \\ &\quad \times \left\{\left|\hat{x}^{\mathrm{L}} \cdot \vec{F}^{\mathrm{L}}\right|^2 - \left|\hat{y}^{\mathrm{L}} \cdot \vec{F}^{\mathrm{L}}\right|^2\right\}, \end{aligned} \tag{15}$$

and $\tilde{b}^{(1)}_{2,-2} = 0$, a peculiarity of the one-photon case. That is, each $\tilde{b}^{(1)}_{l,m}$ coefficient is the product of: a coupling term $|A^{(1)}|^2$ depending on the energy level spacing of the molecule and the spectrum of the electric field, a molecular term expressed in the molecular frame and averaged over all $\hat{k}^{\mathrm{M}}$ directions, and a setup (field and laboratory axes) term expressed in the laboratory frame. Unlike the usual expressions for $\tilde{b}^{(1)}_{l,m}$ (see *e.g.* ref. 4), eqn (12)–(15) provide a rather simple expression for the molecular terms which, as we will now discuss, are simply related to concrete properties of the photoionization vector field $\vec{D}^{\mathrm{M}}(\vec{k})$.

As expected, eqn (12) shows that $b^{(1)}_{0,0}$, which is simply the total cross section, records only the $\hat{k}^{\mathrm{M}}$-averaged value of the magnitude of the field $\vec{D}^{\mathrm{M}}(\vec{k}^{\mathrm{M}})$. More interestingly, eqn (13) shows that $b^{(1)}_{1,0}$ is sensitive to the $\hat{k}^{\mathrm{M}}$-averaged value of the triple product $\hat{k}^{\mathrm{M}} \cdot (\vec{D}^{\mathrm{M}*} \times \vec{D}^{\mathrm{M}})$, which, unlike $b^{(1)}_{0,0}$, depends on the angles between $\vec{k}^{\mathrm{M}}$, $\vec{D}^{\mathrm{M}}$, and $\vec{D}^{\mathrm{M}*}$. The meaning of this quantity can be made evident if we use an appropriate basis for our vector field $\vec{D}^{\mathrm{M}}$. Starting from the unit vectors in spherical coordinates $\hat{k}$, $\hat{\theta}_k$, and $\hat{\varphi}_k$ we define spherical vectors

$$\hat{k}^{\mathrm{M}}_{\pm} = \mp\frac{\hat{\theta}_k \mp i\hat{\varphi}_k}{\sqrt{2}}. \tag{16}$$

If we now write $\vec{D}^{\mathrm{M}}$ in terms of these contravariant helicity-basis vectors,[55]

$$\vec{D}^{\mathrm{M}} = D^{\mathrm{M}}_{+}\hat{k}^{\mathrm{M}}_{+} + D^{\mathrm{M}}_{-}\hat{k}^{\mathrm{M}}_{-} + D^{\mathrm{M}}_{k}\hat{k}^{\mathrm{M}}, \tag{17}$$

then

$$\hat{k}^{\mathrm{M}} \cdot \left(i\vec{D}^{\mathrm{M}*} \times \vec{D}^{\mathrm{M}}\right) = \left|D^{\mathrm{M}}_{+}\right|^2 - \left|D^{\mathrm{M}}_{-}\right|^2. \tag{18}$$

The right hand side of eqn (18) is analogous to the s_3 Stokes parameter for light waves in the circular polarization basis, which describes the difference in intensity between left and right circular polarization.[56] Here we identify the right hand side of eqn (18) with the circular dichroism (CD) of the photoionization vector field $\vec{D}^{\mathrm{M}}$ in the direction $\hat{k}^{\mathrm{M}}$. Indeed, the right hand side of eqn (18) is proportional to the difference between the probability of inducing the transition $|0\rangle \rightarrow |\vec{k}^{\mathrm{M}}\rangle$ using left and right circularly polarized light such that left (+) and right (−) rotations are defined with respect to $\hat{k}^{\mathrm{M}}$ (see Fig. 3). Therefore, the molecular term in $b^{(1)}_{1,0}$ is simply the $\hat{k}^{\mathrm{M}}$-averaged value of the $\vec{k}^{\mathrm{M}}$-specific CD in the molecular frame. Note that the $\vec{k}^{\mathrm{M}}$-specific CD can be non-zero even for achiral molecules, but its average over $\hat{k}^{\mathrm{M}}$ is only non-zero for chiral molecules. Further discussion of $b^{(1)}_{1,0}$ can be found in ref. 30. Remarkably, eqn (18) shows that $b^{(1)}_{1,0}$ depends only on the tangential components of $\vec{D}^{\mathrm{M}}$, namely D^{M}_{+} and D^{M}_{-} (or equivalently D^{M}_{θ} and D^{M}_{φ}). Since the electric field term of $b^{(1)}_{1,0}$ has the same form as the molecular part we can apply a similar procedure and rewrite $b^{(1)}_{1,0}$ as

$$b^{(1)}_{1,0} = \left|A^{(1)}\right|^2 \left\{\frac{1}{6}\sqrt{\frac{3}{4\pi}}\int \mathrm{d}\Omega^{\mathrm{M}}_k \left(\left|D^{\mathrm{M}}_{+}\right|^2 - \left|D^{\mathrm{M}}_{-}\right|^2\right)\right\}\left\{\left|F^{\mathrm{L}}_{+}\right|^2 - \left|F^{\mathrm{L}}_{-}\right|^2\right\}, \tag{19}$$

where

$$\vec{F}^{\mathrm{L}} = F^{\mathrm{L}}_{+}\hat{\varepsilon}^{\mathrm{L}}_{+} + F^{\mathrm{L}}_{-}\hat{\varepsilon}^{\mathrm{L}}_{-} + F^{\mathrm{L}}_{0}\hat{z}^{\mathrm{L}}, \quad \hat{\varepsilon}^{\mathrm{L}}_{\pm} = \frac{\hat{x}^{\mathrm{L}} \pm i\hat{y}^{\mathrm{L}}}{\sqrt{2}} \tag{20}$$

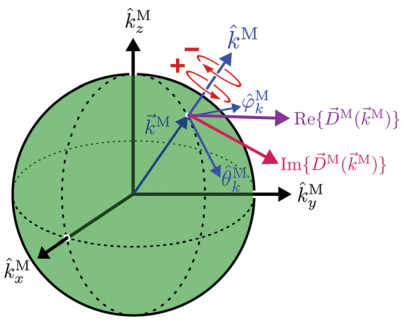

Fig. 3 Sketch of the (complex) photoionization dipole $\vec{D}^{\mathrm{M}}(\vec{k}^{\mathrm{M}}) \equiv \langle\vec{k}^{\mathrm{M}}|\vec{d}|0\rangle$ for a particular value of the photoelectron momentum $\vec{k}^{\mathrm{M}}$. Red circular arrows indicate the direction of left (+) and right (−) circular polarization with respect to $\vec{k}^{\mathrm{M}}$.

§ Note that the expressions (12)–(15) apply for arbitrary polarization of the electric field (in particular for linear polarization along $\hat{z}^{\mathrm{L}}$). The assumption that the field is contained in the xy plane with its major axis along $\hat{x}^{\mathrm{L}}$ or $\hat{y}^{\mathrm{L}}$ simply serves the purpose of reducing the number of non-zero $\tilde{b}^{(1)}_{l,m}$ coefficients.

and $|F_+^{\mathrm{L}}|^2 - |F_-^{\mathrm{L}}|^2$ is the Stokes parameter s_3 in the circular polarization basis.[56]

If we now take the ratio between $b_{1,0}^{(1)}$ [eqn (19)] and $b_{0,0}^{(1)}$ [eqn (12)] we get rid of the coupling term $|A^{(1)}|^2$, and therefore obtain an expression which factorizes into a purely molecular and a purely electric field part,

$$\beta_1^{(1)} \equiv \frac{\sqrt{3}b_{1,0}^{(1)}}{b_{0,0}^{(1)}} = \frac{3}{2}\left\{\frac{\int \mathrm{d}\Omega_k^{\mathrm{M}}\left(|D_+^{\mathrm{M}}|^2 - |D_-^{\mathrm{M}}|^2\right)}{\int \mathrm{d}\Omega_k^{\mathrm{M}}|\vec{D}^{\mathrm{M}}|^2}\right\}\left\{\frac{|F_+^{\mathrm{L}}|^2 - |F_-^{\mathrm{L}}|^2}{|\vec{F}^{\mathrm{L}}|^2}\right\}. \quad (21)$$

As discussed in ref. 57 [see eqn (8)–(10) there], for any number of photons N, we have that $\beta_1^{(N)} \equiv \sqrt{3}b_{1,0}^{(N)}/b_{0,0}^{(N)} = 3j_z^{(N)}/j_r^{(N)}$, where $j_z^{(N)}$ is the net photoelectron current (*i.e.* vector sum of photoelectron currents in all directions) and $j_r^{(N)}$ is the total photoelectron current (*i.e.* sum of magnitudes of photoelectron currents in all directions). Eqn (21) shows that the molecular factor is a measure of the degree of "circular polarization" of the photoionization vector field $\vec{D}^{\mathrm{M}}(\vec{k}^{\mathrm{M}})$ and takes values between −1 and +1, which correspond to the limits $\vec{D}^{\mathrm{M}} = D_+^{\mathrm{M}}\hat{k}_+^{\mathrm{M}}$ (left circularly polarized $\vec{D}^{\mathrm{M}}$) and $\vec{D}^{\mathrm{M}} = D_-^{\mathrm{M}}\hat{k}_-^{\mathrm{M}}$ (right circularly polarized $\vec{D}^{\mathrm{M}}$), respectively. Since the electric field factor is also a measure of the circular polarization of the electric field, then $\beta_1^{(1)} = 3j_z^{(1)}/j_r^{(1)}$ is given by the product of the $\hat{k}^{\mathrm{M}}$-averaged "circular polarization" of the photoionization vector field $\vec{D}^{\mathrm{M}}(\vec{k}^{\mathrm{M}})$ and the circular polarization of the ionizing electric field. Clearly, for a known electric field, $\beta_1^{(1)}$ is a measure of the $\hat{k}^{\mathrm{M}}$-averaged "circular polarization" of $\vec{D}^{\mathrm{M}}(\vec{k}^{\mathrm{M}})$. Finally, eqn (21) shows that $|\beta_1^{(1)}| \leq 1.5$, with the maximal value taking place for circularly polarized light and a "circularly polarized" $\vec{D}^{\mathrm{M}}$ vector field, or equivalently, a purely longitudinal $\vec{B}^{\mathrm{M}} \equiv i\vec{D}^{\mathrm{M}\star} \times \vec{D}^{\mathrm{M}}$ vector field.

Moving on to the next coefficient, eqn (14) shows that, complementarily to $b_{0,0}^{(1)}$ and $b_{1,0}^{(1)}$, which depend on the magnitude and on the tangential components of $\vec{D}^{\mathrm{M}}$, respectively, the coefficient $b_{2,0}^{(1)}$ depends on the projection of $\vec{D}^{\mathrm{M}}$ along $\hat{k}^{\mathrm{M}}$, *i.e.* on its radial component D_k^{M} [see eqn (17)]. We can also consider the ratio between $b_{2,0}^{(1)}$ and $b_{0,0}^{(1)}$ to get rid of the coupling term, and obtain the asymmetry parameter,¶

$$\beta_2^{(1)} \equiv \frac{\sqrt{5}b_{2,0}^{(1)}(k)}{b_{0,0}^{(1)}(k)} = \frac{1}{2}\left\{3\frac{\int \mathrm{d}\Omega_k^{\mathrm{M}}|D_k^{\mathrm{M}}|^2}{\int \mathrm{d}\Omega_k^{\mathrm{M}}|\vec{D}^{\mathrm{M}}|^2} - 1\right\}\left\{3\frac{|F_z^{\mathrm{L}}|^2}{|\vec{F}^{\mathrm{L}}|^2} - 1\right\}. \quad (22)$$

which satisfies the well known fact[40] that the values of $\beta_2^{(1)}$ for linear polarization along z and circular polarization in the xy plane are related to each other by a factor of −2, *i.e.* $\beta_2^{(1,\mathrm{circ})} = -\beta_2^{(1,\mathrm{lin})}/2$. More interestingly, we see that $\beta_2^{(1)}$ is a linear function of the molecular property

$$R \equiv \frac{\int \mathrm{d}\Omega_k^{\mathrm{M}}|D_k^{\mathrm{M}}|^2}{\int \mathrm{d}\Omega_k^{\mathrm{M}}|\vec{D}^{\mathrm{M}}|^2}, \quad 0 \leq R \leq 1, \quad (23)$$

which measures to what extent the vector field $\vec{D}^{\mathrm{M}}(\vec{k}^{\mathrm{M}})$ is a radial field and takes values between 0 and 1, corresponding to the limits $\vec{D}^{\mathrm{M}} = D_+^{\mathrm{M}}\hat{k}_+^{\mathrm{M}} + D_-^{\mathrm{M}}\hat{k}_-^{\mathrm{M}}$ (tangential field) and $\vec{D}^{\mathrm{M}} = D_k^{\mathrm{M}}\hat{k}$ (radial field), respectively. Fig. 4 shows $\beta_2^{(1)}$ as a function of R for linear ($\vec{F}^{\mathrm{L}} = \mathrm{F}_z\hat{z}^{\mathrm{L}}$) and circular polarization ($\vec{F}^{\mathrm{L}} = F_{\pm}\hat{\varepsilon}_{\pm}$) along with the angular distributions obtained in the limits R = 0 (tangential $\vec{D}^{\mathrm{M}}$) and R = 1 (radial $\vec{D}^{\mathrm{M}}$). We can see that for both linearly and circularly polarized fields, a predominantly tangential field $\vec{D}^{\mathrm{M}}$ will yield most photoelectrons with directions perpendicular to the electric field, while a predominantly radial field $\vec{D}^{\mathrm{M}}$ will yield most photoelectrons with directions parallel to the electric field.

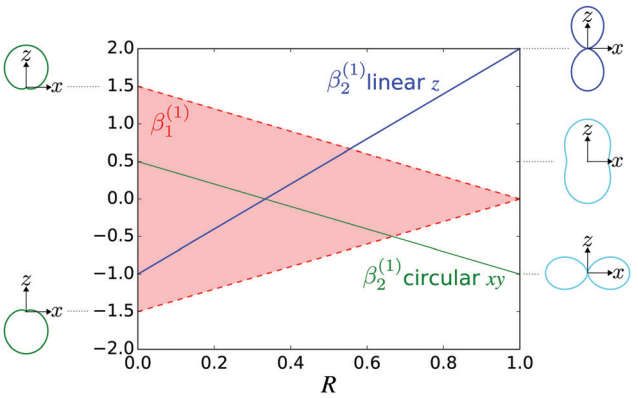

Fig. 4 The relation between $\beta_2^{(1)}$ and the molecular property R, which measures how radial the photoionization dipole field $\vec{D}^{\mathrm{M}}(\vec{k}^{\mathrm{M}}) = \langle \vec{k}^{\mathrm{M}}|\vec{d}^{\mathrm{M}}|0\rangle$ is in average for a given k [see eqn (22) and (23)], for the case of linear polarization along $\hat{z}$ (blue line) and circular polarization in the xy plane (green line). The red shaded area shows the range of values that $\beta_1^{(1)}$ can take for a given value of $\beta_2^{(1)}$ (and correspondingly of R) for the circularly polarized case [see eqn (24)]. $\beta_1^{(1)}$ is zero for linear polarization. The insets on the left show the angular distributions for the extreme values $\beta_1^{(1)} = \pm 1.5$ and $\beta_2^{(1)} = 0.5$ obtained for circular polarization. The insets on the right show the angular distributions for $\beta_1^{(1)} = 0$ (for simplicity) and $\beta_2^{(1)} = -1$ (bottom), $\beta_2^{(1)} = 0.5$ (center), and $\beta_2^{(1)} = 2$ (top), which are the values reached for linear and circular polarizations in the limits R = 0 (tangential $\vec{D}^{\mathrm{M}}$) and R = 1 (radial $\vec{D}^{\mathrm{M}}$).

Fig. 4 also shows the range of values that $\beta_1^{(1)}$ can take as a function of R for light circularly polarized in the xy plane. Using the expressions for $b_{0,0}^{(1)}$, $b_{1,0}^{(1)}$, and $b_{2,0}^{(1)}$ in eqn (12), (14), and (19), and taking into account that $|D_+|^2 + |D_-|^2 \geq |D_+|^2 - |D_-|^2$, one can show that for circularly polarized light $\beta_1^{(1)}$ and $\beta_2^{(1)}$ satisfy the inequality (see ESI†)

$$\left|\beta_1^{(1)}\right| \leq 1 + \beta_2^{(1,\mathrm{circ})} = \frac{3}{2}(1 - R), \quad (24)$$

where we used $\beta_2^{(1,\mathrm{circ})} \equiv (1 - 3R)/2$ as follows from eqn (22) and (23) for circularly polarized light. This inequality follows naturally from the fact that, for circularly polarized light, values of R close to one indicate that the field $\vec{D}(\vec{k})$ is (in average)

¶ The factor of $\sqrt{3}$ in eqn (21) and $\sqrt{5}$ in eqn (22) are included to recover the ratio obtained when the expansion is done in terms of Legendre polynomials (instead spherical harmonics), as is usual for the cylindrically symmetric cases when the light is either linearly polarized along z or circularly polarized in the xy plane.

mostly radial and therefore the tangential components along with $\beta_1^{(1)}$ are very small. On the contrary, values of R close to zero indicate that the field $\vec{D}(\vec{k})$ has (in average) a very small radial component, which means that the field is mostly tangential and can *potentially* display a large dichroism $|D_+|^2 - |D_-|^2$. The maximum value of $|\beta_1^{(1)}| = 1.5$ and requires $\beta_2^{(1,\mathrm{circ})} = 0.5$ and $R = 0$, *i.e.* $\vec{D}^{\mathrm{M}}(\vec{k}^{\mathrm{M}})$ purely tangential *and* perfectly "circularly polarized". As explained in ref. 57 [eqn (9) and (10)], the net photoelectron current (*i.e.* the vector sum of all photoelectron currents) is given by $j_z^{\mathrm{L}}(k) = \sqrt{4\pi/3}kb_{1,0}^{(1)}(k)$ and the total photoelectron current (*i.e.* the sum of the magnitudes of all photoelectron currents) is given by $j_r(k) = \sqrt{4\pi}kb_{0,0}^{(1)}(k)$. Therefore, the maximum value of the ratio of net photoelectron current to total current is $|j_z|/j_r = 1/2$. Note that eqn (24) can also be derived exclusively from the condition that the angular distribution $W^{\mathrm{L}}(\vec{k}^{\mathrm{L}})$ [eqn (2)] is positive for every $\vec{k}^{\mathrm{L}}$.

In practice, the values of $\beta_1^{(1)}$ and $\beta_2^{(1)}$ typically measured or calculated are far from these extreme values. For example, Fig. 3 of ref. 47 shows that for the HOMO orbital of camphor, photoelectrons in the range of 0–60 eV‖ display $0 < \beta_2^{(1,\mathrm{lin})} < 1$. From this we can deduce that $1/3 < R < 2/3$ (see Fig. 4 here). That is, the field $\vec{D}^{\mathrm{M}}(\vec{k}^{\mathrm{M}})$ has a balanced mixture of radial and tangential components. Furthermore, Fig. 3 of ref. 47 also shows that $|\beta_1^{(1)}| \leq 0.2$, which is well below the maximum value $|\beta_1^{(1)}| = 1$ allowed for $R = 1/3$ (see Fig. 4 here). This indicates that while $\vec{D}^{\mathrm{M}}(\vec{k}^{\mathrm{M}})$ has a significant tangential component, it is still far from being perfectly "circularly polarized". Nevertheless, this remnant of "circular polarization" in $\vec{D}^{\mathrm{M}}(\vec{k}^{\mathrm{M}})$ is enough to yield very significant enantio-sensitive signals. From the behavior of $\beta_2^{(1,\mathrm{lin})}$ as a function of energy (see Fig. 3 in ref. 47) we can also deduce that R has an overall tendency to increase with photoelectron energy. That is, $\vec{D}^{\mathrm{M}}(\vec{k}^{\mathrm{M}})$ tends to become more and more radial for increasing photoelectron energies. This is in agreement with the fact that for a plane wave continuum $\vec{D}^{\mathrm{M}}(\vec{k}^{\mathrm{M}})$ is parallel to $\vec{k}^{\mathrm{M}}$ and also with the usual decrease of $|\beta_1^{(1)}|$ with increasing photoelectron energy.

An important difference between $\beta_1^{(1)}$ and $\beta_2^{(1)}$ is that while $\beta_1^{(1)}$ encodes the average magnitude *and sign* of the "circular" component of the field $\vec{D}^{\mathrm{M}}$, the coefficient $\beta_2^{(1)}$ encodes only the average magnitude of the radial component of the field $\vec{D}^{\mathrm{M}}$, but not its sign, *i.e.* it doesn't keep track of whether that radial component points inwards or outwards. This is a plausible explanation of why $\beta_1^{(1)}$ is more sensitive than $\beta_2^{(1)}$ to molecular structure details. This is complementary to the explanation in terms of sines ($\beta_1^{(1)}$) and cosines ($\beta_2^{(2)}$) of phase-shifts differences provided by the partial-wave approach.[41]

Eqn (15) shows that, up to constants, $\tilde{b}_{2,2}^{(1)}$ differs from $b_{2,0}^{(1)}$ only in the electric field factor, which in the case of $\tilde{b}_{2,2}^{(1)}$ yields the s_1 Stokes parameter in the linear polarization basis.[56] That is, $\tilde{b}_{2,2}^{(1)}$ and $b_{2,0}^{(1)}$ reveal the same information about the photoionization vector field $\vec{D}^{\mathrm{M}}(\vec{k}^{\mathrm{M}})$ and differ only on the electric field information they encode. This is a general property of $\tilde{b}_{l,m}$ coefficients with the same value of l and corresponding to the same quantum pathway. It reflects the fact that such coefficients differ only on their laboratory frame vectors [see *e.g.* eqn (9) and (10)] but not on their molecular vectors (photoelectron momentum and transition dipoles), and therefore they involve the same molecular rotational invariants.

‖ The notation used in the figures of ref. 47 is defined in eqn (1) there.

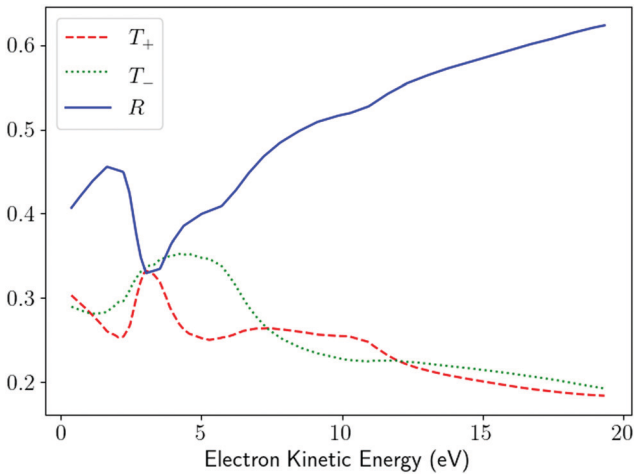

Fig. 5 T_+, T_-, and R [eqn (25) and (26)] as a function of the photoelectron energy for photoionization of alanine from the HOMO orbital. The curves were reconstructed from the values of $\beta_1^{(1)}$ and $\beta_2^{(1)}$ reported in Fig. 9 and 10 of ref. 58 for conformer 3 and $\sigma = 1$.

While so far we have discussed $\beta_1^{(1)}$ and $\beta_2^{(1)}$ in terms of the $\hat{k}^{\mathrm{M}}$-averaged magnitudes of the components of $\vec{D}^{\mathrm{M}}$ [eqn (17), (21), and (22)], it is also interesting to note that for a circularly polarized field $\vec{F}^{\mathrm{L}} = F_\sigma \hat{\varepsilon}_\sigma^{\mathrm{L}}$ with $\sigma = \pm 1$ [see eqn (20)], eqn (12)–(14) can be inverted to reconstruct the $\vec{k}^{\mathrm{M}}$-averaged magnitudes of the components of $\vec{D}^{\mathrm{M}}$ using the measured values of $\beta_1^{(1)}$ and $\beta_2^{(1,\mathrm{circ})}$. Such procedure yields

$$T\pm \equiv \frac{\int \mathrm{d}\Omega_k^{\mathrm{M}} \left|D_\pm^{\mathrm{M}}\right|^2}{\int \mathrm{d}\Omega_k^{\mathrm{M}} \left|\vec{D}^{\mathrm{M}}\right|^2} = \frac{1}{3}\left(1 \pm \sigma\beta_1^{(1)} + \beta_2^{(1,\mathrm{circ})}\right), \tag{25}$$

$$R \equiv \frac{\int \mathrm{d}\Omega_k^{\mathrm{M}} \left|D_k^{\mathrm{M}}\right|^2}{\int \mathrm{d}\Omega_k^{\mathrm{M}} \left|\vec{D}^{\mathrm{M}}\right|^2} = \frac{1}{3}\left(1 - 2\beta_2^{(1,\mathrm{circ})}\right), \tag{26}$$

where $0 \leq T_\pm \leq 1$, $0 \leq R \leq 1$, and $T_+ + T_- + R = 1$. As an example, Fig. 5 shows the values of T_+, T_-, and R as a function of the photoeletron energy for ionization from the HOMO orbital of alanine and reconstructed from the corresponding values of $\beta_1^{(1)}$ and $\beta_2^{(1)}$ reported in ref. 58 for the conformer 3. In agreement with the previous discussion of the results in ref. 47, we see that R tends to increase while T_+ and T_- tend to decrease as the photoelectron energy increases. Unlike the usual figures for $\beta_1^{(1)}$ and $\beta_2^{(1)}$, which are a statement about the PAD, Fig. 5 is a statement about the geometrical properties of the underlying photoionization vector field $\vec{D}^{\mathrm{M}}(\vec{k})$.

5 PECD in resonantly enhanced two-photonionization

We begin by rewriting eqn (9) as

$$\tilde{b}^{(2)}_{l,m}(k) = \frac{1}{2}\left|A^{(2)}\right|^2 d^2 |F|^2 \int \mathrm{d}\Omega^{\mathrm{M}}_k \int \mathrm{d}\rho\, \tilde{Y}^m_l(\hat{k}^{\mathrm{L}}) \sin^2\beta \left|\vec{D}^{\mathrm{L}}\cdot\vec{F}^{\mathrm{L}}\right|^2, \quad (27)$$

where we used the shorthand notation $\vec{D}^{\mathrm{M}} \equiv \vec{d}^{\mathrm{M}}_{\hat{k}^{\mathrm{M}},1}$ for the photoionization dipole from the intermediate state, $\vec{F}^{\mathrm{L}} \equiv \vec{F}^{\mathrm{L}}_{\omega_{\mathrm{L}}} = F(1, i\sigma, 0)/\sqrt{2}$, $\sigma = \pm 1$, and we chose the molecular axis so that $\vec{d}^{\mathrm{M}} \equiv \vec{d}^{\mathrm{M}}_{1,0} = d\hat{z}^{\mathrm{M}}$ and therefore $\vec{d}^{\mathrm{L}} = d(\sin\beta\cos\alpha, \sin\beta\sin\alpha, \cos\beta)$ where $\alpha\beta\gamma$ are the Euler angles in the *ZYZ* convention, and in particular β is the angle between the molecular and laboratory $\hat{z}$ axes. This yields $\left|\vec{d}^{\mathrm{L}}\cdot\vec{F}^{\mathrm{L}}\right|^2 = \frac{1}{2}d^2|F|^2\sin^2\beta$. Written like this, the second order coefficients $\tilde{b}^{(2)}_{l,m}(k)$ take the form of the first order coefficients $\tilde{b}^{(1)}_{l,m}$ for an anisotropic (in this case anti-aligned) sample with an orientation distribution given by $w(\beta) \propto \sin^2\beta$ and an initial state $|1\rangle$ instead of $|0\rangle$ (see also ref. 11, 30 and 58). Such anisotropy gives a certain preference to the z components of the molecular vectors. Performing the orientation averaging according to ref. 46, the expressions for the total absorption $b^{(2)}_{0,0}$, and for the enantio-sensitive terms $b^{(2)}_{1,0}$ and $b^{(2)}_{3,0}$ yield (see ESI† and ref. 17)

$$b^{(2)}_{0,0} = C\left\{\frac{1}{3}\frac{1}{\sqrt{4\pi}}\int \mathrm{d}\Omega^{\mathrm{M}}_k \left|\vec{D}^{\mathrm{M}}_{\mathrm{eff}(0,0)}\right|^2\right\}, \quad (28)$$

$$b^{(2)}_{1,0} = \sigma C\left\{\frac{1}{6}\sqrt{\frac{3}{4\pi}}\int \mathrm{d}\Omega^{\mathrm{M}}_k \left[\hat{k}^{\mathrm{M}}\cdot\left(i\vec{D}^{\mathrm{M}*}_{\mathrm{eff}(1,0)}\times\vec{D}^{\mathrm{M}}_{\mathrm{eff}(1,0)}\right)\right]\right\}, \quad (29)$$

$$= \sigma C\left\{\frac{1}{6}\sqrt{\frac{3}{4\pi}}\int \mathrm{d}\Omega^{\mathrm{M}}_k \left[\vec{K}^{\mathrm{M}}_{1,0}\cdot\left(i\vec{D}^{\mathrm{M}*}\times\vec{D}^{\mathrm{M}}\right)\right]\right\}\frac{\sqrt{3}}{5}, \quad (30)$$

$$b^{(2)}_{3,0} = \sigma C\left\{\frac{1}{35\sqrt{3}}\sqrt{\frac{7}{16\pi}}\int \mathrm{d}\Omega^{\mathrm{M}}_k \left[\vec{K}^{\mathrm{M}}_{3,0}\cdot\left(i\vec{D}^{\mathrm{M}*}\times\vec{D}^{\mathrm{M}}\right)\right]\right\}, \quad (31)$$

where $C \equiv d^2|F|^4|A^{(2)}|^2$ is a common factor to all $b^{(2)}_{l,m}$ coefficients that simply encodes the bound-bound transition and the second order character of the process, and the expressions for $\vec{D}^{\mathrm{M}}_{\mathrm{eff}(0,0)}$, $\vec{D}^{\mathrm{M}}_{\mathrm{eff}(1,0)}$, $\vec{K}^{\mathrm{M}}_{1,0}$, and $\vec{K}^{\mathrm{M}}_{3,0}$ are given below. We wrote eqn (28)–(31) so that we can draw a parallel to the corresponding eqn (12) and (13) in the one-photon case. Eqn (28) and (29) show that we can recover the forms obtained in the one-photon case if we introduce effectively stretched photoionization dipoles given by

$$\vec{D}^{\mathrm{M}}_{\mathrm{eff}(0,0)} \equiv \sqrt{\frac{3}{10}}\left(D^{\mathrm{M}}_x, D^{\mathrm{M}}_y, \frac{2}{\sqrt{3}}D^{\mathrm{M}}_z\right), \quad (32)$$

and

$$\vec{D}^{\mathrm{M}}_{\mathrm{eff}(1,0)} \equiv \frac{1}{\sqrt{5}}\left(D^{\mathrm{M}}_x, D^{\mathrm{M}}_y, 2D^{\mathrm{M}}_z\right). \quad (33)$$

In view of the discussion in Section 4, eqn (28) shows that $b^{(2)}_{0,0}$ records the $\hat{k}^{\mathrm{M}}$-averaged magnitude of an effective photoionization dipole $\vec{D}^{\mathrm{M}}_{\mathrm{eff}(0,0)}(\hat{k}^{\mathrm{M}})$. Similarly, eqn (29) shows that $b^{(2)}_{1,0}$ records the "circular polarization" [see eqn (18)] or equivalently the $\hat{k}^{\mathrm{M}}$-averaged value of the $\hat{k}^{\mathrm{M}}$-specific CD of an effective photoionization dipole $\vec{D}^{\mathrm{M}}_{\mathrm{eff}(1,0)}(\hat{k}^{\mathrm{M}})$. Their ratio, $\beta^{(2)}_1 \equiv \sqrt{3}b^{(2)}_{1,0}/b^{(2)}_{0,0}$, can be interpreted as the average "circular polarization" of $\vec{D}^{\mathrm{M}}_{\mathrm{eff}(1,0)}$ normalized with respect to the average magnitude of $\vec{D}^{\mathrm{M}}_{\mathrm{eff}(0,0)}$.

In the case of $b^{(2)}_{3,0}$, quadratic terms in k_z (see ESI†) hinder a straightforward interpretation of the integrand in terms of an effectively stretched $\vec{D}^{\mathrm{M}}$. However, like $b^{(1)}_{1,0}$ and $b^{(2)}_{1,0}$ [eqn (13) and (30)], eqn (31) shows that $b^{(2)}_{3,0}$ depends on the photoionization dipole $\vec{D}^{\mathrm{M}}(\hat{k}^{\mathrm{M}})$ only through the $\hat{k}^{\mathrm{M}}$-dependent field[29,30]

$$\vec{B}^{\mathrm{M}} \equiv i\vec{D}^{\mathrm{M}*}\times\vec{D}^{\mathrm{M}}, \quad (34)$$

and we can therefore attempt an interpretation of $b^{(2)}_{3,0}$ in terms of $\vec{B}^{\mathrm{M}}$ directly.

We have already found rigorous physical interpretations for the projections $\hat{A}^{\mathrm{M}}\cdot\vec{B}^{\mathrm{M}}$ for $\hat{A}^{\mathrm{M}} = \hat{x}^{\mathrm{M}}, \hat{y}^{\mathrm{M}}, \hat{z}^{\mathrm{M}}, \hat{k}^{\mathrm{M}}$ (see ref. 30 and Section 4). In these cases we found that $\hat{A}^{\mathrm{M}}\cdot\vec{B}^{\mathrm{M}}$ yields the $\hat{k}^{\mathrm{M}}$-specific CD associated to the transition $|0\rangle \rightarrow |\vec{k}^{\mathrm{M}}\rangle$ for light circularly polarized with respect to the axis $\hat{A}^{\mathrm{M}}$ (see Fig. 3). In fact, this interpretation is valid for an arbitrary $\hat{A}^{\mathrm{M}}$. To see this, note that for a given $\hat{A}^{\mathrm{M}}$ one can always build $\hat{A}^{\mathrm{M}}$-dependent unit vectors $\hat{e}^{\mathrm{M}}_{\pm}$ associated to positive and negative rotations around $\hat{A}^{\mathrm{M}}$, write $\vec{D}^{\mathrm{M}} = D^{\mathrm{M}}_+\hat{e}^{\mathrm{M}}_+ + D^{\mathrm{M}}_-\hat{e}^{\mathrm{M}}_- + D^{\mathrm{M}}_0\hat{A}^{\mathrm{M}}$ and obtain $\hat{A}^{\mathrm{M}}\cdot\vec{B}^{\mathrm{M}} = \left|\vec{D}^{\mathrm{M}}_+\right|^2 - \left|\vec{D}^{\mathrm{M}}_-\right|^2$. This scalar product is evidently maximized for $\hat{A}^{\mathrm{M}} = \hat{B}^{\mathrm{M}}$, and therefore the direction of $\vec{B}^{\mathrm{M}}$ indicates the axis with respect to which the $\hat{k}^{\mathrm{M}}$-specific CD is maximal. The magnitude of $\vec{B}^{\mathrm{M}}$ is then the magnitude of such maximal $\hat{k}^{\mathrm{M}}$-specific CD. Light circularly polarized with respect to axes perpendicular to $\vec{B}^{\mathrm{M}}$ yield zero $\hat{k}^{\mathrm{M}}$-specific CD.

While eqn (13) shows that $b^{(1)}_{1,0}$ involves the projection of $\vec{B}^{\mathrm{M}}$ on the radial vector $\hat{k}^{\mathrm{M}}$, eqn (30) and (31) show that $b^{(2)}_{1,0}$ and $b^{(2)}_{3,0}$ involve the projection of $\vec{B}^{\mathrm{M}}$ on the vector fields $\vec{K}^{\mathrm{M}}_{1,0}$ and $\vec{K}^{\mathrm{M}}_{3,0}$, respectively, defined as (see ESI†)

$$\vec{K}^{\mathrm{M}}_{1,0} \equiv \frac{1}{\sqrt{3}}\left(2\hat{k}^{\mathrm{M}} - \frac{k^{\mathrm{M}}_z}{k}\hat{z}^{\mathrm{M}}\right), \quad (35)$$

$$\vec{K}^{\mathrm{M}}_{3,0} \equiv \frac{\sqrt{3}}{2}\left\{\left[1 - 5\left(\frac{k^{\mathrm{M}}_z}{k}\right)^2\right]\hat{k}^{\mathrm{M}} + 2\frac{k^{\mathrm{M}}_z}{k}\hat{z}^{\mathrm{M}}\right\}, \quad (36)$$

and shown in Fig. 6 as a function of θ^{M}_k on a plane parallel to k^{M}_z. The integrations over all $\hat{k}^{\mathrm{M}}$ directions in eqn (29) and (31) tell us that $b^{(2)}_{1,0}$ and $b^{(2)}_{3,0}$ record the extent to which the vector field $\vec{B}^{\mathrm{M}}$ resembles the vector fields $\vec{K}^{\mathrm{M}}_{1,0}$ and $\vec{K}^{\mathrm{M}}_{3,0}$, respectively, and therefore record structural information about $\vec{B}^{\mathrm{M}}$. Such information can be made more explicit by expanding $\vec{K}^{\mathrm{M}}_{1,0}$, $\vec{K}^{\mathrm{M}}_{3,0}$, and $\vec{B}^{\mathrm{M}}$ in terms of vector spherical harmonics[59] $\vec{Y}^{\mathrm{M}}_{l,m}(\hat{k}^{\mathrm{M}}) \equiv Y^m_l(\hat{k}^{\mathrm{M}})\hat{k}^{\mathrm{M}}$, $\vec{\Psi}^{\mathrm{M}}_{l,m}(\hat{k}^{\mathrm{M}}) \equiv k\vec{\nabla}Y_{l,m}(\hat{k}^{\mathrm{M}})\Big/\sqrt{l(l+1)}$, and $\vec{\Phi}^{\mathrm{M}}_{l,m}(\hat{k}^{\mathrm{M}}) \equiv \hat{k}^{\mathrm{M}}\times\vec{\Psi}^{\mathrm{M}}_{l,m}\Big/\sqrt{l(l+1)}$,

$$\vec{K}^{\mathrm{M}}_{1,0}\left(\hat{k}^{\mathrm{M}}\right) = \frac{2}{3}\sqrt{\frac{\pi}{15}}\left[5\sqrt{5}\,\vec{Y}^{\mathrm{M}}_{0,0}(\hat{k}^{\mathrm{M}}) - 2\vec{Y}^{\mathrm{M}}_{2,0}(\hat{k}^{\mathrm{M}}) - \sqrt{6}\vec{\Psi}^{\mathrm{M}}_{2,0}(\hat{k}^{\mathrm{M}})\right], \quad (37)$$

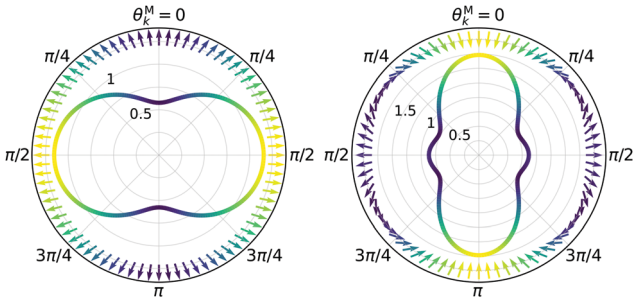

Fig. 6 Direction (arrows) and magnitude (color and solid lines) of the vector fields $\vec{K}^{M}_{1,0}(\hat{k}^{M})$ and $\vec{K}^{M}_{3,0}(\hat{k}^{M})$ in eqn (35) and (36).

$$\vec{K}^{M}_{3,0}\left(\hat{k}^{M}\right) = 2\sqrt{\frac{\pi}{5}}\left[-\sqrt{3}\,\vec{Y}^{M}_{2,0}\left(\hat{k}^{M}\right) + \sqrt{2}\vec{\Psi}^{M}_{2,0}\left(\hat{k}^{M}\right)\right], \tag{38}$$

$$\vec{B}^{M}(\vec{k}^{M}) = \sum_{l,m}\Big[\mathscr{B}^{Y}_{l,m}(k)\,\vec{Y}^{M}_{l,m}(\hat{k}^{M}) + \mathscr{B}^{\Psi}_{l,m}(k)\vec{\Psi}^{M}_{l,m}(\hat{k}^{M}) + \mathscr{B}^{\Phi}_{l,m}(k)\vec{\Phi}^{M}_{l,m}(\hat{k}^{M})\Big]. \tag{39}$$

Replacing eqn (34), (37)–(39) in eqn (30) and (31) and using the orthonormality relations for the vector spherical harmonics,[59] we obtain

$$b^{(2)}_{1,0} = \frac{\sigma C}{30\sqrt{15}}\left(5\sqrt{5}\mathscr{B}^{Y}_{0,0} - 2\mathscr{B}^{Y}_{2,0} - \sqrt{6}\mathscr{B}^{\Psi}_{2,0}\right), \tag{40}$$

$$b^{(2)}_{3,0} = \frac{\sigma C}{10\sqrt{105}}\left(-\sqrt{3}\mathscr{B}^{Y}_{2,0} + \sqrt{2}\mathscr{B}^{\Psi}_{2,0}\right). \tag{41}$$

That is, while in the one-photon case $b^{(1)}_{1,0}$ encodes $\mathscr{B}^{Y}_{0,0}$ (because $\hat{k}^{M} \propto \vec{Y}^{M}_{0,0}$), in the two-photon case $b^{(2)}_{1,0}$ and $b^{(2)}_{3,0}$ encode $\mathscr{B}^{Y}_{0,0}$, $\mathscr{B}^{Y}_{2,0}$, and $\mathscr{B}^{\Psi}_{2,0}$. This motivates looking for a third linearly independent equation to solve for $\mathscr{B}^{Y}_{0,0}$, $\mathscr{B}^{Y}_{2,0}$, and $\mathscr{B}^{\Psi}_{2,0}$. This is delivered by the equation for $b'^{(2)}_{1,0}$ for the complementary process where the first photon is linearly polarized along $\hat{z}^{L}$ and the second photon is circularly polarized in the $\hat{x}^{L}\hat{y}^{L}$ plane (see ESI†),

$$b'^{(2)}_{1,0} = \frac{\sigma C}{30\sqrt{15}}\left(5\sqrt{5}\mathscr{B}^{Y}_{0,0} + 4\mathscr{B}^{Y}_{2,0} + 2\sqrt{6}\mathscr{B}^{\Psi}_{2,0}\right). \tag{42}$$

Eqn (42) together with (40) and (41) yield

$$\mathscr{B}^{Y}_{0,0} = \frac{2\sqrt{3}}{\sigma C}\left(2b^{(2)}_{1,0} + b'^{(2)}_{1,0}\right), \tag{43}$$

$$\mathscr{B}^{Y}_{2,0} = \frac{2\sqrt{15}}{\sigma C}\left(-b^{(2)}_{1,0} - \sqrt{21}b^{(2)}_{3,0} + b'^{(2)}_{1,0}\right), \tag{44}$$

$$\mathscr{B}^{\Psi}_{2,0} = \frac{\sqrt{30}}{\sigma C}\left(-\sqrt{3}b^{(2)}_{1,0} + 2\sqrt{7}b^{(2)}_{3,0} + \sqrt{3}b'^{(2)}_{1,0}\right). \tag{45}$$

These coefficients quantify the contributions of the fields $\vec{Y}^{M}_{0,0}(\hat{k}^{M}) \propto \hat{k}^{M}$, $\vec{Y}^{M}_{2,0}(\vec{k}^{M}) \propto (3\cos^2\theta^{M}_{k} - 1)\hat{k}^{M}$, and $\vec{\Psi}^{M}_{2,0}(\hat{k}^{M}) \propto -\cos\theta^{M}_{k}\sin\theta^{M}_{k}\hat{\theta}^{M}_{k}$ to the total field $\vec{B}^{M}(\hat{k}^{M})$ [eqn (34)]. Eqn (43)–(45) thus clearly show how structural information of the molecular field $\vec{B}^{M}(\hat{k}^{M})$ can be reconstructed from photoelectron angular distributions resulting from an initially isotropic sample of chiral molecules.

In Table VII of ref. 11, the resonantly enhanced two-photon ionization of camphor with circularly polarized light yields** $\beta^{(2)}_{1} \equiv \sqrt{3}b^{(2)}_{1,0}\big/b^{(2)}_{0,0} = 0.075$ and $\beta^{(2)}_{3} \equiv \sqrt{7}b^{(2)}_{3,0}\big/b^{(2)}_{0,0} = -0.02$. While this is not enough to reconstruct $\mathscr{B}^{Y}_{0,0}$, $\mathscr{B}^{Y}_{2,0}$, and $\mathscr{B}^{\Psi}_{2,0}$ using eqn (43)–(45), it is enough to state that $\int d\Omega^{M}_{k}\left(\vec{K}^{M}_{1,0}\cdot\vec{B}^{M}\right)\Big/\int d\Omega^{M}_{k}\left(\vec{K}^{M}_{3,0}\cdot\vec{B}^{M}\right) = \beta^{(2)}_{1}/\sqrt{21}\beta^{(2)}_{3} = -0.82$. That is, the overlap between $\vec{K}^{M}_{1,0}$ and $\vec{B}^{M}$ is only slightly smaller than that between $\vec{K}^{M}_{3,0}$ and $\vec{B}^{M}$.

6 Conclusions

We have presented an alternative approach to obtain expressions for the $b^{(N)}_{l,m}$ coefficients of photoelectron angular distributions resulting from perturbative N-photon ionization of isotropic samples. These expressions are explicitly written in terms of products between the molecular rotational invariants and the setup rotational invariants, and do not invoke a partial wave expansion for the scattering wave function. The molecular rotational invariants are expressed in terms of vector products involving only molecular vectors: transition dipoles and the photoelectron momentum labeling a particular scattering state in the molecular frame. The setup rotational invariants are expressed in terms of vector products involving only setup vectors: field polarization vectors and detection axes. Our expressions reveal how the molecular rotational invariants are coupled to the setup rotational invariants. Knowledge of this coupling can assist the interpretation and design of future experiments and simulations. The standard expressions can be recovered by subsequent expansion of the scattering wave function if needed.

With the help of this methodology we found that, independently of the polarization of the field, enantio-sensitive $b^{(N_1,N_2)}_{l,m}$ coefficients resulting from interference between pathways involving N_1 and N_2 photons have odd $l + N_1 + N_2$.

The application of our methodology to the case of one-photon ionization $|0\rangle \rightarrow |\vec{k}\rangle$ reveals a clear meaning for the molecular information encoded in each of the $b^{(1)}_{l,m}$ coefficients, which is otherwise obscured in the usual (and equivalent) formulation in terms of partial waves: $b^{(1)}_{0,0}$ encodes the average magnitude of the photoionization dipole $\vec{D}(\vec{k}) \equiv \langle\vec{k}|\vec{d}|0\rangle$; $b^{(1)}_{1,0}$ encodes the average radial component of the field $\vec{B} \equiv i\vec{D}^{*}\times\vec{D}$,[29,30] which in turn encodes the average 'circular dichroism' of $\vec{D}(\vec{k})$ and depends only on its transverse components; and $b^{(1)}_{2,0}$ encodes the average radial component of $\vec{D}(\vec{k})$. The averages are taken with respect to the direction of the photoelectron momentum $\vec{k}$ in the molecular frame. $b^{(1)}_{1,0}$ is sensitive to a single coefficient of the vector spherical harmonic expansion of $\vec{B}(\vec{k})$.

We also derived expressions for the coefficients $b^{(2)}_{0,0}$, $b^{(2)}_{1,0}$, and $b^{(2)}_{3,0}$ relevant for two-photon resonantly enhanced

** The notation used in Table VII of ref. 11 is defined in eqn (8) there.

ionization $|0\rangle \rightarrow |1\rangle \rightarrow |\vec{k}\rangle$ of isotropic chiral samples with circularly polarized light. The coefficients $b^{(2)}_{0,0}$ and $b^{(2)}_{1,0}$ have analogous interpretations to those found in the one-photon case provided one takes into account an effective anisotropic stretching of the photoionization dipoles. $b^{(2)}_{1,0}$ and $b^{(2)}_{3,0}$ yield structural information about the propensity field $\vec{B} \equiv i\vec{D}^* \times \vec{D}$,[29,30] which encodes the $\vec{k}$-specific circular dichroism. In particular they depend only on three coefficients of the vector spherical harmonic expansion of $\vec{B}(\vec{k})$. These coefficients can be solved for in terms of $b^{(2)}_{1,0}$, $b^{(2)}_{3,0}$, and $b^{'(2)}_{1,0}$, where the latter corresponds to the process where the first photon is linearly polarized.

Further application of the methodology introduced here can be found in ref. 39, where it is used to analyze the enantio-sensitive asymmetry recently found in the photoelectron angular distributions resulting from interaction of chiral samples with a field containing ω and 2ω frequencies linearly polarized orthogonal to each other.[18,54]

Conflicts of interest

There are no conflicts to declare.

Acknowledgements

A. F. O. and O. S. gratefully acknowledge the MEDEA Project, which has received funding from the European Union's Horizon 2020 Research and Innovation Programme under the Marie Skłodowska-Curie Grant Agreement No. 641789. A. F. O. and O. S. gratefully acknowledge support from the DFG SPP 1840 ''Quantum Dynamics in Tailored Intense Fields'' and DFG Grant No. SM 292/5-2. A. F. O. gratefully acknowledges grants supporting his research at ICFO: Agencia Estatal de Investigación (the R&D project CEX2019-000910-S, funded by MCIN/AEI/10.13039/501100011033, Plan Nacional FIDEUA PID2019-106901GB-I00, FPI), Fundació Privada Cellex, Fundació Mir-Puig, Generalitat de Catalunya (AGAUR Grant No. 2017 SGR 1341, CERCA program), and EU Horizon 2020 Marie Skłodowska-Curie grant agreement no. 101029393.

Notes and references

1 A. Stolow, A. E. Bragg and D. M. Neumark, *Chem. Rev.*, 2004, **104**, 1719–1758.
2 A. Stolow and J. G. Underwood, *Advances in Chemical Physics*, John Wiley & Sons, Ltd, 2008, pp. 497–584.
3 K. L. Reid, *Mol. Phys.*, 2012, **110**, 131–147.
4 B. Ritchie, *Phys. Rev. A*, 1976, **13**, 1411.
5 I. Powis, *J. Chem. Phys.*, 2000, **112**, 301–310.
6 N. Böwering, T. Lischke, B. Schmidtke, N. Müller, T. Khalil and U. Heinzmann, *Phys. Rev. Lett.*, 2001, **86**, 1187–1190.
7 V. Ulrich, S. Barth, S. Joshi, U. Hergenhahn, E. Mikajlo, C. J. Harding and I. Powis, *J. Phys. Chem. A*, 2008, **112**, 3544–3549.
8 M. H.-M. Janssen and I. Powis, *Phys. Chem. Chem. Phys.*, 2013, **16**, 856–871.
9 L. Nahon, G. A. Garcia and I. Powis, *J. Electron Spectrosc. Relat. Phenom.*, 2015, **204**(Part B), 322–334.
10 C. Lux, M. Wollenhaupt, T. Bolze, Q. Liang, J. Köhler, C. Sarpe and T. Baumert, *Angew. Chem., Int. Ed.*, 2012, **51**, 5001–5005.
11 C. S. Lehmann, R. B. Ram, I. Powis and M. H.-M. Janssenn, *J. Chem. Phys.*, 2013, **139**, 234307.
12 I. Dreissigacker and M. Lein, *Phys. Rev. A*, 2014, **89**, 053406.
13 S. Beaulieu, A. Ferré, R. Géneaux, R. Canonge, D. Descamps, B. Fabre, N. Fedorov, F. Légaré, S. Petit, T. Ruchon, V. Blanchet, Y. Mairesse and B. Pons, *New J. Phys.*, 2016, **18**, 102002.
14 S. Beaulieu, A. Comby, A. Clergerie, J. Caillat, D. Descamps, N. Dudovich, B. Fabre, R. Géneaux, F. Légaré, S. Petit, B. Pons, G. Porat, T. Ruchon, R. Taïeb, V. Blanchet and Y. Mairesse, *Science*, 2017, **358**, 1288–1294.
15 A. Comby, S. Beaulieu, M. Boggio-Pasqua, D. Descamps, F. Légaré, L. Nahon, S. Petit, B. Pons, B. Fabre, Y. Mairesse and V. Blanchet, *J. Phys. Chem. Lett.*, 2016, **7**, 4514–4519.
16 S. Beaulieu, A. Comby, D. Descamps, B. Fabre, G. A. Garcia, R. Géneaux, A. G. Harvey, F. Légaré, Z. Mašín, L. Nahon, A. F. Ordonez, S. Petit, B. Pons, Y. Mairesse, O. Smirnova and V. Blanchet, *Nat. Phys.*, 2018, **14**, 484–489.
17 A. F. Ordonez and O. Smirnova, *Phys. Rev. A*, 2018, **98**, 063428.
18 P. V. Demekhin, A. N. Artemyev, A. Kastner and T. Baumert, *Phys. Rev. Lett.*, 2018, **121**, 253201.
19 R. E. Goetz, C. P. Koch and L. Greenman, *Phys. Rev. Lett.*, 2019, **122**, 013204.
20 J. C. Tully, R. S. Berry and B. J. Dalton, *Phys. Rev.*, 1968, **176**, 95–105.
21 D. Dill, *J. Chem. Phys.*, 1976, **65**, 1130–1133.
22 R. R. Lucchese, G. Raseev and V. McKoy, *Phys. Rev. A*, 1982, **25**, 2572–2587.
23 S. N. Dixit and V. McKoy, *J. Chem. Phys.*, 1985, **82**, 3546–3553.
24 N. Chandra, *J. Phys. B: At. Mol. Phys.*, 1987, **20**, 3405.
25 D. J. Leahy, K. L. Reid and R. N. Zare, *J. Chem. Phys.*, 1991, **95**, 1757–1767.
26 K. L. Reid, D. J. Leahy and R. N. Zare, *J. Chem. Phys.*, 1991, **95**, 1746–1756.
27 J. G. Underwood and K. L. Reid, *J. Chem. Phys.*, 2000, **113**, 1067–1074.
28 P. Decleva, M. Stener and D. Toffoli, *Molecules*, 2022, **27**, 2026.
29 A. F. Ordonez, D. Ayuso, P. Decleva and O. Smirnova, 2021, arXiv:2106.14264 [physics].
30 A. F. Ordonez and O. Smirnova, *Phys. Rev. A*, 2019, **99**, 043417.
31 M. V. Berry, *Proc. R. Soc. A*, 1984, **392**, 45–57.
32 R. Resta, *J. Phys.: Condens. Matter*, 2000, **12**, R107–R143.
33 S. Tsesses, E. Ostrovsky, K. Cohen, B. Gjonaj, N. H. Lindner and G. Bartal, *Science*, 2018, **361**, 993–996.
34 L. Du, A. Yang, A. V. Zayats and X. Yuan, *Nat. Phys.*, 2019, **15**, 650–654.
35 E. Pisanty, G. J. Machado, V. Vicuña-Hernández, A. Picón, A. Celi, J. P. Torres and M. Lewenstein, *Nat. Photonics*, 2019, **13**, 569–574.
36 R. Gutiérrez-Cuevas and E. Pisanty, *J. Opt.*, 2021, **23**, 024004.

37 Y. Tokura and N. Kanazawa, *Chem. Rev.*, 2021, **121**, 2857–2897.
38 G. Sundaram and Q. Niu, *Phys. Rev. B*, 1999, **59**, 14915–14925.
39 A. F. Ordonez and O. Smirnova, *Phys. Chem. Chem. Phys.*, 2022, **24**, 7264.
40 K. L. Reid, *Annu. Rev. Phys. Chem.*, 2003, **54**, 397–424.
41 I. Powis, *Advances in Chemical Physics*, John Wiley & Sons, Inc., 2008, vol. 138, pp. 267–329.
42 M. Stener, G. Fronzoni, D. D. Tomasso and P. Decleva, *J. Chem. Phys.*, 2004, **120**, 3284–3296.
43 A. Giardini, D. Catone, S. Stranges, M. Satta, M. Tacconi, S. Piccirillo, S. Turchini, N. Zema, G. Contini, T. Prosperi, P. Decleva, D. D. Tommaso, G. Fronzoni, M. Stener, A. Filippi and M. Speranza, *ChemPhysChem*, 2005, **6**, 1164–1168.
44 C. J. Harding and I. Powis, *J. Chem. Phys.*, 2006, **125**, 234306.
45 D. D. Tommaso, M. Stener, G. Fronzoni and P. Decleva, *ChemPhysChem*, 2006, **7**, 924–934.
46 D. L. Andrews and T. Thirunamachandran, *J. Chem. Phys.*, 1977, **67**, 5026–5033.
47 M. Stener, D. Di Tommaso, G. Fronzoni, P. Decleva and I. Powis, *J. Chem. Phys.*, 2006, **124**, 024326.
48 Z. Lu, J. E. Oakman, Q. Hu and R. E. Continetti, *Mol. Phys.*, 2008, **106**, 595–606.
49 M. Staniforth, S. Daly, K. L. Reid and I. Powis, *J. Chem. Phys.*, 2013, **139**, 064304.
50 M. M. Rafiee Fanood, M. H.-M. Janssen and I. Powis, *J. Chem. Phys.*, 2016, **145**, 124320.
51 C. Lux, M. Wollenhaupt, C. Sarpe and T. Baumert, *ChemPhysChem*, 2015, **16**, 115–137.
52 D. M. Brink and G. R. Satchler, *Angular Momentum*, Clarendon Press, Oxford, 2nd edn, 1968.
53 M. M. Rafiee Fanood, I. Powis and M. H.-M. Janssen, *J. Phys. Chem. A*, 2014, **118**, 11541–11546.
54 P. V. Demekhin, *Phys. Rev. A*, 2019, **99**, 063406.
55 D. A. Varschalovich, A. N. Moskalev and V. K. Khersonskii, *Quantum Theory of Angular Momentum*, World Scientific, 1988.
56 J. D. Jackson, *Classical Electrodynamics*, John Wiley & Sons, 3rd edn, 1999.
57 A. F. Ordonez and O. Smirnova, *Phys. Rev. A*, 2019, **99**, 043416.
58 R. E. Goetz, T. A. Isaev, B. Nikoobakht, R. Berger and C. P. Koch, *J. Chem. Phys.*, 2017, **146**, 024306.
59 R. G. Barrera, G. A. Estevez and J. Giraldo, *Eur. J. Phys.*, 1985, **6**, 287.